QM/MM Molecular Dynamics Simulation of the Structure of Hydrated Fe(II) and Fe(III) Ions

Tawun Remsungnen and Bernd M. Rode*

Department of Theoretical Chemistry, Institute of General, Inorganic and Theoretical Chemistry, University of Innsbruck, A-6020 Innsbruck, Austria

Received: September 16, 2002; In Final Form: January 17, 2003

The hydration shell structure of Fe(II) and Fe(III) ions in their high spin state has been studied by combined ab initio quantum mechanical/molecular mechanical (QM/MM) molecular dynamics simulations, in which the ion and its first hydration sphere were treated at the Hartree−Fock ab initio quantum mechanical level, whereas ab initio generated pair plus three-body potentials were employed for the remaining system. The coordination number in the first hydration shell is 6 for both Fe(II) and Fe(III) ions. The second hydration shell contains 12.4 and 13.4 water molecules for Fe(II) and Fe(III) ions, respectively, in good agreement with the experimental values. The residence time of a water molecule in the second hydration shells of Fe(II) and Fe(III) is 24 and 48 ps, respectively. The complex configuration and ligand orientations observed in this study prove that many-body effects play an important role in the hydration of both Fe(II) and Fe(III) ions. The hydration energies computed from the simulation are within experimental error boundaries of estimated hydration enthalpies of the ions.

1. Introduction

Molecular dynamics (MD) and Monte Carlo (MC) computer simulation techniques are well-established tools of computational chemistry and other areas of science.[1−5] However, their success strongly depends on the interaction potential models employed in the system.[6] Empirical potentials, which are normally parametrized with respect to the experimental data, can yield reasonable results for the structural and dynamical properties. However, there are some problems when such empirical potentials are applied. They cannot, for example, describe configurations far from equilibrium and/or transition states assumed in reaction mechanisms, and they do not allow bonds to form or break.[7] Therefore, the most common pairwise potentials are parametrized with respect to the interaction energies obtained from ab initio molecular orbital calculations. This approach, however, suffers from an overestimation of the binding energy, as result of neglecting the nonadditive behavior of polarization.[8] This problem, which affects both structural and energetic results,[9] has been widely examined for polar system such as water and becomes much more important in the case of interaction between ions and polar molecules, particularly of highly charged ions.[10−12] In comparison to the neglect of *n*-body effects, the neglect of electron correlation in the potential functions is only a very minor error source, in particular, when dealing with strong interaction of cation−solvent type. To compensate the many-body problems, ab initio effective pair potentials based on the polarizable continuum model (PCM) have been proposed.[14] This approach includes many-body effects in an average way relying on a continuum polarizable model for the solvent and could yield the correct experimental first hydration number of 6 for both Fe(II) and Fe(III) in water.[14] However, especially in the hydration shell of ions, some contributions can be attractive, others repulsive, and averaging them is ambiguous and may lead to a failure of effective pair potentials[15] A more rigorous and exact approach is to supplement the pair potential function with many-body terms. In several cases, three-body potentials calculated by ab initio methods have reproduced properly structural and dynamical parameters,[9,12,16−21] but the complexity of the calculation procedures increases with the order of n-body terms to be determined[22] by ab initio methods, and they are, therefore, hardly feasible for larger systems and *n* larger than 3. Moreover, because of the asymptotic behavior of the many-body potential, fittings of ab initio energy surfaces to a simple analytical formula is a difficult trial-and-error task even for three-body potential functions. This difficulty to describe the potential energy by analytical functions calls for ab initio quantum mechanical (QM) methods to calculate interactions between particles within the simulated system. This approach allows to calculate rather accurate interaction potentials for any instantaneous configuration, whereby many-body effects are included up to the degree determined by the number of particles included in the QM region. An ab initio quantum mechanical treatment of the entire system is still not feasible at present, except for rather small model system with far too few particles to properly model a liquid system. Even the use of the strongly simplified BLYP-DFT approach in Car−Parrinello type simulation limits the number of ligands to 30−60 molecules, which, apart from the methodical error sources, introduces a high artificial symmetry through periodic boundary conditions. Consequently, a hybrid approach, the combined quantum mechanical/molecular mechanical (QM/MM) method was introduced,[23−28] with the concept that the quantum mechanical treatment is applied to a selected, chemically relevant region, and the rest of the system is described at a less computationally demanding level, such as simple force fields or ab initio constructed analytical potentials.

Because of the important role of Fe(II) and Fe(III) in chemical and biological processes numerous experimental and theoretical

* To whom correspondence should be addressed. E-mail: Bernd.M.Rode@uibk.ac.at. Phone: +43(0)512/507-5161. Fax: +43(0)512/507-2714.

10.1021/jp027007i CCC: $25.00
Published on Web 03/07/2003

TABLE 1: Optimized Parameters for Pair Potential Functions and Three-Body Correction Functions

pair	A kcal mol^{-1} Å^a	B kcal mol^{-1} Å^b	C kcal mol^{-1} Å^c	D kcal mol^{-1} Å^d	a,b,c,d
Fe(II)−O	−12278.7433	27740.47670	−19611.86942	4303.3413	5,6,8,12
Fe(II)−H	1604.398697	−3585.38635	2642.78747	−680.76223	5,6,8,12
Fe(III)−O	−11456.49984	81418.48201	−86802.13176	23768.78161	5,7,8,12
Fe(III)−H	818.31445	2434.12043	1098.56636	1333.06548	5,7,8,12
3-body	A_1 kcal mol^{-1} Å^{-4}	A_2 Å^{-1}	A_3 Å^{-1}	A_4 kcal mol^{-1} Å	A_5 kcal mol^{-1} Å
Fe(II)	0.38343	0.00477	0.61822	0.05454	0.38639
Fe(III)	59.53987	0.44852	2.19552	−0.01713	−0.03374

[a] The net charges, q on Fe(II), Fe(III), 0, and H are 2.0, 3.0, −0.6596 and 0.3298, respectively.

studies have focused on the hydration of these ions.[12,14,29−32,35,36] Effective pair potentials[12] and potentials based on the polarizable continuum model for the solvent[14] have been used in MD simulations of Fe(II) and Fe(III) ions in water. These potentials deliver smaller cation−water binding energies than those obtained from ab initio calculations and, thus, yield the correct experimental hydration number of 6 for both ions. This number was confirmed by a classical MD study based on ab initio pair plus three-body potential functions.[36,37] A slightly distorted octahedral arrangement of the water molecules in the first hydration shell was obtained, with ion−oxygen distances between 2.10 and 2.18 Å for Fe(II) and 1.98 and 2.05 Å for Fe(III). The large and well-defined second peaks that were observed in the ion−oxygen radial distribution functions (RDF) represent a distinct second hydration shell for both Fe(II) and Fe(III) ions. The number of water ligands in this second hydration shell obtained from MC[35] and classical MD[36,37] were ∼13 for Fe(II) and ∼15 for Fe(III), whereas the experimental information[32] indicates these numbers to be near 12, in both cases. It seemed most important, therefore, to apply the high-level QM/MM method to these systems in order to obtain structural and dynamical data for these two ions at the highest level of accuracy of presently feasible simulation techniques.

2. Details of Calculation

The pair potentials for Fe(II)−water and Fe(III)−water are taken from refs 36 and 37 and are composed as expressed by eq 1

$$\Delta E^{2bd} = \sum_{ij}\left(\frac{A_{ij}}{r_{ij}^{\,a}} + \frac{B_{ij}}{r_{ij}^{\,b}} + \frac{C_{ij}}{r_{ij}^{\,c}} + \frac{D_{ij}}{r_{ij}^{\,d}} + \frac{q_i q_j}{r_{ij}}\right) \qquad (1)$$

where i denotes the Fe(II) or Fe(III) ion and j oxygen and hydrogen atoms, respectively, and r_{ij} is the distance between atoms i and j. All parameters for pair potentials are given in Table 1. The three-body correction terms, to be added to the pair potentials for both ions are expressed in eq 2

$$\Delta E_{3bd} = \left[A_1 \exp(-A_2 r_{FeO_1} - A_2 r_{FeO_2} - A_3 r_{O_1O_2}) - \frac{A_4}{r_{FeO_1}} - \frac{A_4}{r_{FeO_2}} - \frac{A_5}{r_{O_1O_2}}\right][(CL - r_{FeO_1})^2 (CL - r_{FeO_2})^2] \qquad (2)$$

A_n are fitting parameters, and O_1 and O_2 refer to the oxygens of the first and second water molecule. r_{FeO_1} and r_{FeO_2} and $r_{O_1O_2}$ refer to distances between ion to the oxygen of the first and second water molecule, respectively, whereas $r_{O_1O_2}$ refers to the distance between the oxygens of the first and second water molecules. CL represents the cutoff limit set to 6.0 Å, beyond which the three-body contributions are negligible. The optimized parameters of the three-body functions are listed in Table 1.

Classical molecular dynamics simulations of one ion plus 499 water molecules in a periodic cube at a temperature of 298.16 K are performed first. The density of the system was assumed to be the same as that of pure water (0.997 g cm^{-3}). Radial cutoff distances of 3.0 and 5.0 Å were adopted for non-Coulombic interactions between H atoms and between O and H atoms, respectively. All other pair interaction were cutoff at half of the box length (12.345 Å). In addition a reaction field[2] was established to properly account for long-term Coulombic interactions. Because the BJH−CF2 water model[38,39] used in this simulation allows explicit hydrogen movements, the time step was set to 0.2 fs. The water box, subject to periodic boundary conditions, was equilibrated for 200 000 time steps (40 ps) in the NVT-ensemble, temperature being controlled by the velocity-scaling method with a relaxation time of 100 fs.[40] The combined QM/MM-MD simulations[41,42] were performed subsequently, using the equilibrium configuration obtained from the classical simulations. Because the computational effort (i.e., CPU time) for ab initio force calculations is extremely high, the size of the QM region could not be too large. Therefore, the diameter of the first hydration shell of ions obtained from the classical simulations was used to define the size of this region, leading to a diameter of 7.2 Å. The remaining water molecules were described by pair plus three-body potential functions as in the classical simulations. An interval of 0.2 Å was allowed for the transition region between QM and MM forces and smoothing functions were applied in this region.[41] The hybrid QM/MM-MD simulations made use of the same ECP basis sets[36,37] for Fe(II) and Fe(III) ions and DZP basis sets[43] for water molecule as employed in the construction of pair and three-body functions. The systems were reequilibrated for 25 000 time steps (5 ps) and the following 50 000 time steps (10 ps) were used to collect configurations for the evaluation of structural data.

3. Results and Discussion

3.1. Structure of Hydration Shells of Fe(II) and Fe(III) Ions. The Fe−O and Fe−H RDFs and their running integration numbers and coordination number distributions are shown in parts a and b of Figure 1 for Fe(II) and Fe(III), respectively. The first hydration shell is represented by a first Fe−O peak, at 2.10 and 2.02 Å for Fe(II) and Fe(III) ions, respectively, and it is well separated from the second shell that appears between 3.65 and 5.10 Å (maximum at 4.50 Å) for the Fe(II) ion and between 3.6 and 5.0 Å (maximum at 4.30 Å) for the Fe(III) ion. In both Fe−O RDFs, a third diffuse peak is observed (from 5.1 to 7.50 Å for Fe(II) ion and 5.0 to 7.50 Å for Fe(III) ion) which could correspond to a third hydration shell or at least to considerable structural effects on bulk water surrounding the hydrated Fe(II) and Fe(III) ions. The RDFs seem to indicate that the third hydration shell of Fe(II) ion is more clearly structured than that of Fe(III) ion. However, this behavior may be caused by the interplay of pair potential and three-body correction functions, as the cutoff for the latter is set to 6 Å,

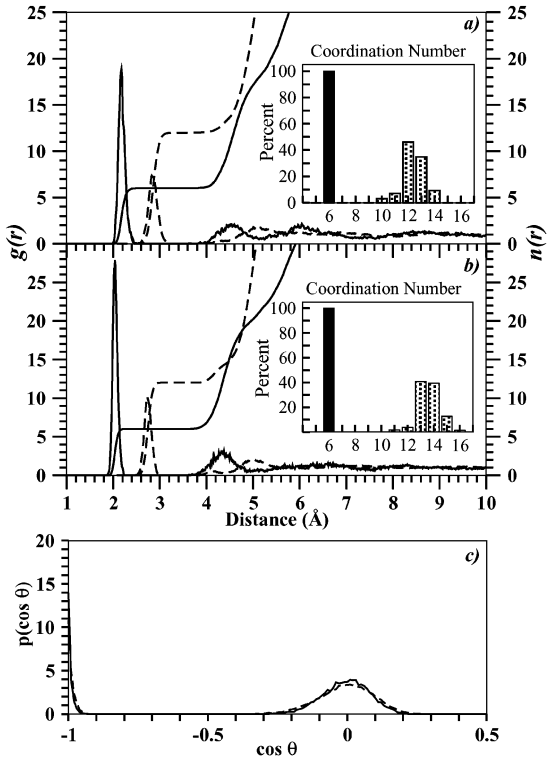

Figure 1. Fe−O (full lines) and Fe−H (dashed lines) RDFs with their corresponding integration numbers and the coordination number distributions in the first (black) and the second (grey) hydration shells for (a) Fe(II)−water and (b) Fe(III)−water. (c) Probability distribution of the cosine of O−Fe−O angle, θ, in the first hydration shell of Fe(II) (dashed line) and Fe(III) (full line), respectively.

rather in the center of the third peak. The more flexible Fe(II) hydration shell may allow more easily artificial pile-up of water molecules near this boundary, and hence, this structural feature should not be considered as very significant. The characteristic values for Fe−O and Fe−H radial distribution functions are listed and compared with results obtained from experiments and other simulations in Table 2.

The probability distributions of the coordination numbers were calculated up to 3.0 Å for the first hydration shells of both ions and up to 5.1 and 5.0 Å for the second hydration shells of Fe(II) and Fe(III) ion, respectively. 100% of the solvates have exactly 6 water molecules in the first hydration shell. The mean coordination numbers for the second hydration shell are 12.4 and 13.4 for Fe(II) and Fe(III), respectively. These numbers are considerably lower than those obtained from classical MD. Obviously, the QM treatment of the first shell improves the description of the second shell, even it is outside the QM region. This has also been observed for other ions (Hg(II), Ni(II), Mn(II), Cr(III), and Co(III))[41,42,44] and can be explained by the changes induced in the first shell ligands geometry and orientation and thus changed binding opportunities for second shell water molecules. These numbers indicate that all water molecules in the first shell form hydrogen bonds with two water molecules in the second shell. These second shell coordination numbers come very close to available experimental data, but when comparing, one should keep in mind that these experimental data were obtained for more than 1.5 M concentrated solutions, where counterion effects can reach a significant extent, whereas our simulation corresponds to a much lower concentration, comparable to those relevant for biological Fe-containing systems. In Figure 1c, the probability distribution of cos θ is shown, with θ representing the O−Fe−O angle. The distribution

TABLE 2: Bond Distances, Coordination Numbers, and Binding Energies for Fe(II)−Water and Fe(III)−Water Complexes/Solvates

characteristic[a]	method[b]/reference	Fe^{2+}	Fe^{3+}
R_1^{max}/R_1^{min} (Å)	MD(QM/MM)/This work	2.10/2.40	2.02/2.20
R_1^{max}/R_1^{min} (Å)	MD(3BD)/ref 36	2.15/2.40	2.05/2.35
R_{FeO}^{expt} (Å)	ND/ref 31	2.01	
	ND/ref 30	2.12	
	XD,ND,EX/ref 32	2.10−2.28	1.99−2.05
R_1^{max} (Å)	MD(EP)/ref 12	2.11−2.27	1.98−2.11
	MD(PCM)/ref 14	2.15	2.03
	MC(PCM)/ref 35	2.10	1.96
R_2^{max}/R_2^{min} (Å)	MD(QM/MM)/This work	4.50/5.20	4.30/5.00
R_2^{max}/R_2^{min} (Å)	MD(3BD)/ref 36	4.60/5.20	4.30/5.10
N_{R_1}/N_{R_2}	MD(QM/MM)/This work	6.0/12.4	6.0/13.4
	MD(3BD)/ref 36	6.0/12.9	6.0/15.1
	MC(PCM)/ref 35	6.0/13.0	6.0/15.0
$N^{expt}{}_{R_1}/N^{expt}{}_{R_2}$	ref 32	6.0/12.0	6.0/12.0
ΔE_{hyd}^{qm} kcal/mol	MD(QM/MM)/This work	500 ± 10	1100 ± 10
ΔE_{hyd}^{3bd} kcal/mol	MD(3BD)/ref 36	520 ± 20	1120 ± 15
ΔH_{hyd}^{expt} kcal/mol	ref 45	471	1066

[a] R_1^{max} and R_1^{min} denote the distances of the first RDF maxima and minima, respectively, whereas R_{FeO}^{expt} denotes the experimental Fe−O distances. N_{R_1} and N_{R_2} denote the first and second shell coordination number from simulations, whereas $N_{R_1}^{expt}$ and $N_{R_2}^{expt}$ denote the experimental first and second coordination numbers. ΔE_{hyd}^{qm} and ΔE_{hyd}^{3bd} denote the energies of hydration from simulations, whereas ΔE_{hyd}^{expt} denotes the experimental enthapies. [b] The methods are abbreviated as follows: ND, neutron diffraction; XD, X-ray diffraction; EX, EXAFS; MD, molecular dynamics; MC, Monte Carlo. Some potential models adopted to the classical simulation are referred to by following abbreviations: 3BD, classical pair potential plus 3-body correction functions; EP, empirical potential; PCM, polarizable continuum model.

displays only two peaks centered at −1.0 and 0.0 for both Fe(II) and Fe(III), corresponding to an octahedral complex. Another interesting feature for the comprehensive discussion of the structure of the hydrated ions and their influence on the solvent structure is the orientation and configuration of the water molecules in the hydration sphere. The angle ζ, defined by the Fe−O axis and the dipole vector of water, has been used to characterize the orientation of water molecules, and its relative cosine distribution within the first and second hydration shells is shown in Figure 2. Water molecules in the first hydration shell show a clear ion-induced orientation. The distribution displays only peaks centered at −1.0 for both Fe(II) and Fe(III). The differences between ligand orientation of Fe(II) and Fe(III) become much more observable in the second shell, where Fe(III) still exerts a strong influence of the ion on the ligand binding, whereas in the case of Fe(II), slowly decaying values until −0.2 indicate that H bonding between first and second shell is the dominating structure-forming factor.

The hydration energies, ΔE_{hyd}^{QM}, calculated for Fe(II) and Fe(III) ions were computed as the sum of all of interaction energies between ion and water molecules including the reaction field energy and are also shown in Table 2. The experimental hydration enthalpies,[45] ΔH_{hyd}^{exp}, agree within 10%, i.e., within the limits of experimental accuracy, with the energies obtained by the QM/MM-MD simulations.

3.2. Water Exchange Process. The residence time, τ_{res}, of water molecules in the second hydration shell was estimated following the procedure of Impey et al.[46] The experimental[32] values of the binding time of water molecules in the first hydration shell of Fe(II) and Fe(III) aqueous solution were determined in the range of 10^{-6}−10^{-7} and 10^{-3}−10^{-5} s, respectively, i.e., several orders of magnitude longer than our total simulation time. Consequently, no water molecule ex-

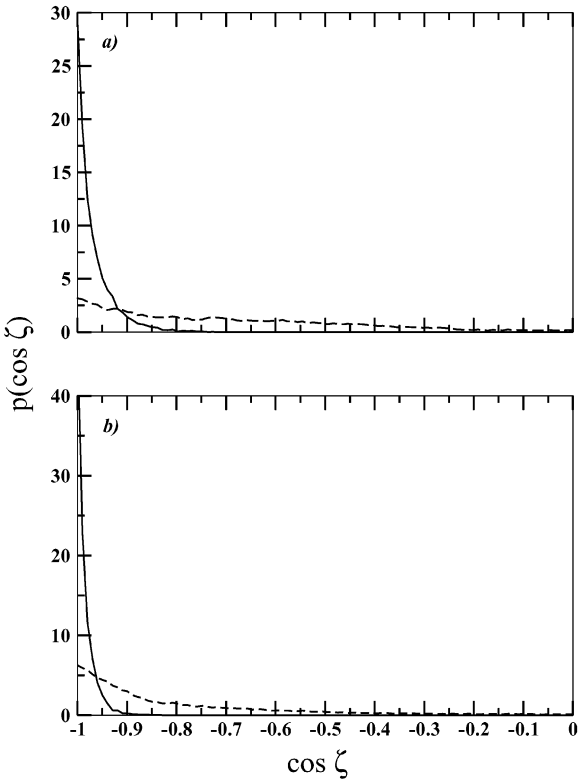

Figure 2. Probability distribution of the cosine of the angle ζ between the oxygen-ion vector and the dipole vector of water in the first (full line) and second (dashed line) hydration shells form the simulation for (a) Fe(II) and (b) Fe(III) ions, respectively.

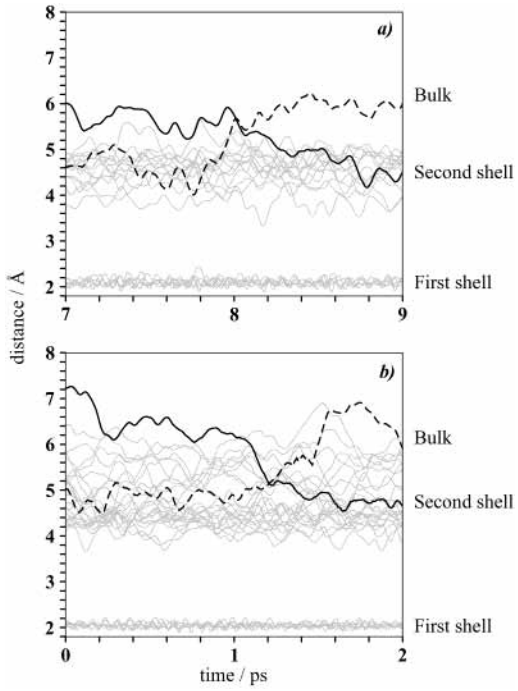

Figure 3. Examples of second shell exchange processes: Plot of Fe−O distance versus time for water molecules in first and second hydration shells in the simulations of (a) Fe(II) and (b) Fe(III) ions in aqueous solution. Entering (solid line) and leaving (dashed line) water molecules are highlighted.

change between first and second hydration shell was observed during the whole simulation. However, exchange between second shell ligands and bulk takes place much more readily as shown in Figure 3. The ligand residence time obtained by QM/MM-MD simulations for Fe(II) and Fe(III) in the second hydration shell is 24 and 48 ps, respectively, considerably higher than obtained from classical MD (10 and 32 ps).[36,37] For Fe(III), experimental estimations[31] for τ_{res} are available in the range of $10^{-10}-10^{-11}$ s and are thus in full agreement with our value, whereas for Fe(II), only data for τ_{res} for hydrated Ni(II) and Co(II) with 10.3 and 4.5 ps are available from PCM potential simulations for comparison.[47] Within the total simulation time of 10 ps, 4 exchange processes were observed for Fe(II) and 3 processes for Fe(III) ion, as shown in the examples of Figure 3. In the case of Fe(II), a rather simultaneous interchange mechanism is observed, whereas in the case of Fe(III), a first associative step is followed by the expulsion of another ligand. The number of observed exchange processes with the given average number of second shell ligands is consistent with the mean residence times calculation according to Impey: for Fe(II), an observed exchange occurred every 2.5 ps, and τ_{res} of 24 ps with 12.4 ligands predicts an exchange every 2.1 ps. For Fe(III), the corresponding values are 3.3 (observed time between the 3 exchange processes) and 3.6 ps (predicted by τ_{res} of 48 ps and 13.4 ligands).

4. Conclusion

The hydration structure obtained from QM/MM-MD simulations for Fe(II) and Fe(III) ions is in very good agreement with the experimental data. Differences to classical MD simulations are observed in ion-ligand distances, ligand orientation, second shell coordination numbers, and the mean residence times of water molecules in the second hydration shell. This clearly indicates that higher-order corrections are important to correctly obtain the properties of hydrated transition metal ions, in particular of their second hydration shell. This is apparently of great importance for characterizing ions of great similarity, i.e., neighboring transition metal ions of the same charge or of the same element different only in the charge as in the present case of Fe(II)/Fe(III).

Acknowledgment. Financial support by the Austrian Science Foundation, project No. 16221 and a scholarship of the Austrian Federal Ministry for Foreign Affairs for T.R. are gratefully acknowledged.

References and Notes

(1) Clementi, E. in *Determination of Liquid Water Structure, Coordination Number of Ions and Solvation for Biological Molecules*; Springer-Verlag: New York, 1976.
(2) Allen M. P.; Tildesley D. J. *Computer Simulation of Liquids*; Clarendon Press: Oxford, U.K., 1987.
(3) Ciccotti, G.; Frenkel, D.; McDonald, I. R. *Simulation of Liquids and Solids. Molecular Dynamics and Monte Carlo Methods in Statistical Mechanics*; North-Holland: Amsterdam, 1987.
(4) Clementi, E.; Corongiu, G. *J. Biol Phys.* **1983**, *11*, 33.
(5) Berendsen, H. J. C. *Comput. Phys. Commun.* **1987**, *44*, 233.
(6) Stone, J. A. *The Theory of Intermolecular Forces*; Clarendon Press: Oxford, U.K., 1996.
(7) McCommon, J. A., Harvey, S. C. Eds.; *Dynamics of Proteins and Nuclei Acids*; Cambridge University Press: London 1987.
(8) Clementi, E.; Corongiu, G.; Jönnson, B.; Romano, S. J. *Chem. Phys.* **1980**, *72*, 260.
(9) Texler, N. R.; Rode, B. M. *J. Chem. Phys.* **1995**, *99*, 15714.
(10) Elrod, N. J.; Berendsen, H. J. C.; Grigera, J. R.; Straatsma, T. P. *J. Chem. Phys.* **1987**, *91*, 6269.
(11) Elrod, N. J.; Saykally, R. J. *Chem. Rev.* **1994**, *94*, 1975.
(12) Curtiss, L. A.; Halley, J. W.; Hautman, J.; Rahman, A. *J. Chem. Phys.* **1987**, *86*, 2319.
(13) Meirtus, S.; Scrocco, E.; Tomasi, J. *Chem. Phys.* **1981**, *55*, 117.
(14) Floris, F.; Persico, M.; Tani, A.; Tomasi, J. *Chem. Phys. Lett.* **1992**, *199*, 518.
(15) Berendsen, H. J. C.; Grigera, J. R.; Straatsma, T. P. *J. Phys. Chem.* **1987**, *91*, 6269.

(16) Marini, G. W.; Texler, N. R.; Rode, B. M. *J. Phys. Chem.* **1996**, *100*, 6808.
(17) Pranowo, H. D.; Rode, B. M. *J. Phys. Chem. A* **1999**, *103*, 4298.
(18) Lybrand, T. P.; Kollman, P. A. *J. Chem. Phys.* **1985**, *83*, 2923.
(19) Rode, B. M.; Islam, S. M. *Z. Naturforsch., Part A* **1991**, *46*, 357.
(20) Ortega-Blake, I.; Novaro, O.; Les', A.; Rybak, S. *J. Chem. Phys.* **1982**, *76*, 5405.
(21) Hannongbua, S.; Kerdcharoen, T.; Rode, B. M. *J. Chem. Phys.* **1992**, *96*, 6945.
(22) Dietrich, J.; Corongiu, G.; Clementi, E. *Chem. Phys. Lett.* **1984**, *112*, 426.
(23) Warshel, A.; Karplus, M. *J. Am. Chem. Soc.* **1972**, *94*, 5612.
(24) Allinger, N. L.; Sprague, J. T. *J. Am. Chem. Soc.* **1973**, *95*, 3893.
(25) Bash, P. A.; Field, M. J.; Karplus, M. *J. Am. Chem. Soc.* **1987**, *109*, 8092.
(26) Gao, J. In *Review of Computational Chemistry*; Lipkowitz, K. B., Boyd, D. B., Eds.; VCH: New York, 1995; Vol. 7, p 119.
(27) Kerdcharoen, T.; Liedl, K. R.; Rode, B. M. *Chem. Phys.* **1996**, *211*, 313.
(28) Tongraar, A.; Liedl, K. R.; Rode, B. M. *J. Phys. Chem. A* **1998**, *286*, 56.
(29) Neilson, G. W.; Enderby, J. E. *Adv. Inorg. Chem.* **1989**, *34*, 195.
(30) Herdman, G. J.; Neilson, G. W. *J. Phy.*: *Condens. Matter* **1992**, *4*, 649.
(31) Herdman, G. J.; Neilson, G. W. *J. Phy.*: *Condens. Matter* **1992**, *4*, 627.
(32) Ohtaki, H.; Radnai, T. *Chem. Rev.* **1993**, *93*, 1157.
(33) Kneifel, C. L.; Friedman, H. L.; Newton, M. D. *Z. Naturfosch.* **1989**, *44A*, 385.
(34) Rustad, J. R.; Hay, B. P. *J. Chem. Phys.* **1995**, *102*, 427.
(35) Degréve, L.; Quintale, C., Jr. *J. Electroanal. Chem.* **1996**, *409*, 25.
(36) Remsungnen, T. Ph.D. Thesis, University Innsbruck, Innsbruck, Austria, 2002.
(37) Remsungnen, T.; Rode, B. M. submitted.
(38) Stillinger, F. H.; Rahman, A. *J. Chem. Phys.* **1978**, *68*, 666.
(39) Bopp, P.; Jancsó, G.; Heinzinger, K. *Chem. Phys. Lett.* **1983**, *98*, 129.
(40) Berendsen, H. J. C.; Postma, J. P. M.; van Gunsteren, W. F.; DiNola, A.; Haak, *J. R. J. Chem. Phys*. **1984**, *81*, 3684.
(41) Yagüe, J. I.; Mohammed, A. M.; Loeffler, H.; Rode, B. M. *J. Phys. Chem. A* **2001**, *105*, 7646.
(42) Inada, Y.; Mohammed, A. M.; Loeffler, H. H.; Rode, B. M. *J. Phys. Chem. A* **2002**, *106*, 6783.
(43) Dunning, T. H., Jr. *J. Chem. Phys.* **1975**, *53*, 2823.
(44) Kritayakornupong, C.; Rode, B. M. submitted.
(45) Marcus, Y. *Ionic Solvation* Wiley: New York, 1985.
(46) Impey, R. W.; Madden, P. A.; McDonald, I. R. *J. Phys. Chem.* **1983**, *87*, 5071.
(47) Chillemi, G.; D'Angelo, P.; Pavel, N. V.; Sanna, N.; Barone, V. *J. Am. Chem. Soc.* **2001**, *124*, 1968.